Non-Hermitian Efimov physics in dissipative three-body systems

Mingyuan Sun [1,2] Chang Liu [3] and Zhe-Yu Shi [4,*]

[1]*State Key Lab of Information Photonics and Optical Communications, Beijing University of Posts and Telecommunications, Beijing 100876, China*

[2]*School of Science, Beijing University of Posts and Telecommunications, Beijing 100876, China*

[3]*Institute for Advanced Study, Tsinghua University, Beijing 100084, China*

[4]*State Key Laboratory of Precision Spectroscopy, East China Normal University, Shanghai 200062, China*

(Received 5 May 2022; revised 2 September 2023; accepted 20 September 2023; published 4 October 2023)

Efimov effect is characterized by an infinite number of three-body bound states following a universal geometric scaling law at two-body resonances. In this paper, we investigate the influence of two-body losses which can be described by a complex scattering length a_c on these states. Interestingly, the non-Hermiticity allows the system to have three-body bound states of energies with nonvanishing imaginary parts and real parts that may exceed the three-body or the atom-dimer scattering threshold. By taking the ^{133}Cs - ^{133}Cs - ^{6}Li system as a concrete example, we calculate the trimer energies by solving the generalized Skorniakov–Ter-Martirosian equation and find such three-body bound states with energies that have positive real parts and obey a generalized geometric scaling law. Remarkably, we also find that in some regions these three-body bound states have longer lifetimes compared with the corresponding two-body bound states. In the absence of other loss mechanisms such as three-atom loss, the lifetimes for these trimer states can tend to infinity. Our work paves the way for the future exploration of few-body bound states in the complex plane.

DOI: 10.1103/PhysRevResearch.5.043010

I. INTRODUCTION

Three identical bosons can form an infinite series of bound states near a two-body resonance which satisfy a universal scaling law and display a discrete scaling symmetry [1]. It is called the Efimov effect and has been generalized to various three-particle systems with different mass ratios and statistics [2–4]. Efimov physics has been observed in a number of cold atom experiments [5–21] as well as in gaseous helium [22]. Conventionally, studies on few-body physics are restricted in dissipationless closed systems. However, dissipation is ubiquitous and naturally leads to the decoherence or decay of quantum states. On the other hand, it can also be used as a tool to engineer exotic new physics in open systems [23–39]. For instance, dissipation can induce correlation in one-dimensional molecular gases [23], a reentrant superfluid transition [32,38], and distinct topological phases with complex energy spectra, which have no Hermitian counterpart in closed systems [24–30,37]. Moreover, it can also be adopted as a probe to detect the equilibrium property of a Hermitian system [34,35]. Thus, one might wonder how dissipation affects few-body physics such as the Efimov effect in a three-body system.

In this work, we shed light on this problem by studying the effect of short-range two-body losses on Efimov bound states. Two-body losses naturally occur in ultracold atom systems, as the two-atom collision process is generically inelastic. It is shown that such short-range two-body losses can be described by a complex scattering length a_c [40,41]. As an analog of the conventional real s-wave scattering length, the complex scattering length characterizes the inelastic scattering process between two atoms and requires the two-body wave function having the asymptotic behavior $\psi(\mathbf{r}) \approx r^{-1} - a_c^{-1}$ for $r \to 0$. In particular, the value a_c^{-1} can be experimentally tuned across the entire upper half of the complex plane by the (optical) Feshbach resonance which couples two ground state atoms to an excited two-atom bound state with a finite lifetime [39,40]. This allows us to go beyond the conventional real scattering length constraint in the few-body calculations and explore Efimov physics in the complex a_c^{-1} plane [42].

In the following, we focus on a three-body system consisting of two heavy identical bosons and one light particle (boson or fermion), which has been extensively studied with no dissipation [2–4,43]. We assume there exist short-range interactions and two-body losses between the heavy boson and the third particle, which can be characterized by a complex scattering length a_c. And the interaction and loss between heavy bosons are set to be zero for simplicity. One advantage of this system is that the scaling factor becomes smaller when the mass ratio between the heavy boson (with mass m_b) and the light particle (with mass m_0) m_b/m_0 increases. This facilitates both the experimental observation and theoretical calculation of the geometric scaling law [19–21]. For example, in the ^{133}Cs - ^{133}Cs - ^{6}Li system, the scaling factor is

*zyshi@lps.ecnu.edu.cn

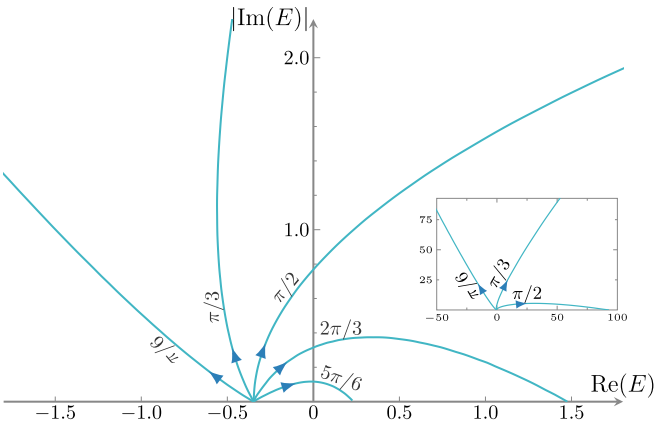

FIG. 1. Energy trajectories of Efimov trimers in the complex plane. For each trajectory, we fix the argument of complex scattering length $\phi = \arg(a_c^{-1})$ and gradually increase its norm $|a_c^{-1}|$ from zero (unitarity) to a positive number. We only show the trimer states that connect to the third-lowest Efimov trimers at unitarity. All the trajectories start from the same unitarity point with $E \approx -0.35$ [all the energies are in units of E_0 with $E_0 = \Lambda^2/(400m_b)$], while they vanish at the three-body branch cut ($E \in \mathbb{R}^+$) for $\phi \geqslant \pi/2$, and at the atom-dimer branch cut ($E \in \{E_d + \Delta E : \Delta E \in \mathbb{R}^+\}$) for $\phi < \pi/2$. We note that the latter scenario is not visible because of its large scale. This will be demonstrated in detail in Fig. 4. Inset is a zoom-out of the same plot.

$e^{2\pi/s_0} \approx 23.7$, compared to 515.0 for three identical bosons. Thus, we calculated the energy spectra of three-body bound states in such a system by solving a generalized Skorniakov–Ter-Martirosian (STM) equation with two-body losses [2,44].

It is worth mentioning that, in the literature, there have been several related works that consider the effects of two-particle loss on Efimov states [45,46]. The main contribution of this work is that, based on a previous work on the two-body inelastic scattering process by two of the authors [41], we are able to treat both the two-body interaction and dissipation on an equal footing by implementing a complex scattering length a_c. This point of view has not been adopted until recently by Zhou and Cui [39]. While in Ref. [39] the three-body problem is solved based on Born-Oppenheimer and adiabatic hyperspherical approximations, in this work we adopt the more strict and formal STM equation subjected to two-particle losses. We also go beyond the restriction $\mathrm{Re}(E) < 0$ of the bound state energies and explore the Efimov states on the entire lower half complex energy plane. This helps reveal the deep holomorphic nature of the contact interaction and two-body loss. For example, by considering the complex derivative of the eigenenergy with respect to a_c^{-1}, we find that it is possible to define the complex Tan's contact [47,48] for certain Efimov states.

Our main result is summarized in Fig. 1. Owing to the two-body losses, the energies of the Efimov trimers are analytically continued from the negative real axis to the complex energy plane. Thus, to display the complex trimer energies as functions of complex a_c, we fix the argument $\phi \equiv \arg(a_c^{-1})$ and gradually increase its norm $|a_c^{-1}|$ from zero to a positive number and plot the trajectories of the energies on the complex plane. First of all, we find that at $|a_c^{-1}| = 0$, or equivalently, $|a_c| = +\infty$, the argument ϕ does not affect the trimer energies. That is to say, the system only has one resonance point even in the presence of two-body losses, i.e., $a_c^{-1} = 0$ [49]. Therefore, all the trajectories start from the same point on the negative real axis, which represents conventional Efimov trimer energy at resonance, and continuously extend to the complex plane for different arguments ϕ. Two different scenarios may occur for the trajectories in the parameter regime $\phi \in [0, \pi]$. For $\phi \geqslant \pi/2$, it ends at the three-body branch cut with a positive energy $E \in \mathbb{R}^+$, and results in an approximate semicircle shape in the complex energy plane. One distinct feature from the conventional Efimov effect is that the energy trajectories do not end at the three-body scattering threshold, i.e., $E = 0$, but are able to go beyond with $\mathrm{Re}(E) > 0$ in the presence of dissipation. As $\phi \to \pi$, the trajectory recovers the Efimov result on the BCS side. On the other hand, for $\phi < \pi/2$, there exists a two-body bound state with complex energy E_d. This energy defines the complex atom-dimer scattering threshold, for no three-body bound state exists on the horizontal ray (atom-dimer branch cut) defined by $\{E \in \mathcal{C} : \mathrm{Re}(E) \geqslant \mathrm{Re}(E_d)$ and $\mathrm{Im}(E) = \mathrm{Im}(E_d)\}$. The energy trajectories in this region extend beyond the atom-dimer scattering threshold with $\mathrm{Re}(E) > \mathrm{Re}(E_d)$ and disappear into a state at the atom-dimer branch cut. As $\phi \to 0$, they again recover the conventional result for Efimov states on the Bose-Einstein condensate (BEC) side.

II. MODEL

Generally speaking, the dynamics of an open system are governed by the Lindblad equation. For a three-particle system, the dynamics are greatly simplified and the Lindblad equation for the three-particle density matrix is fully described by a non-Hermitian Hamiltonian [41]

$$\mathcal{H} = \frac{\mathbf{p}_0^2}{2m_0} + \sum_{j=1,2} \frac{\mathbf{p}_j^2}{2m_\mathrm{b}} + \sum_{j=1,2} g_c \delta(\mathbf{r}_0 - \mathbf{r}_j), \tag{1}$$

where $\mathbf{r}_0$ and $\mathbf{p}_0$ denote the position and momentum of the light particle, while $\mathbf{r}_j$ and $\mathbf{p}_j$ $(j = 1, 2)$ denote the position and momentum of the two heavy bosons. The coupling constant g_c is complex and is related to the complex scattering length a_c by the renormalization relation

$$\frac{1}{g_c} = \frac{m_r}{2\pi a_c} - \frac{1}{V} \sum_{\mathbf{k}} \frac{2m_r}{k^2}, \tag{2}$$

with $m_r = 1/(m_0^{-1} + m_b^{-1})$ being the two-body reduced mass. We note that $\mathrm{Im}(g_c)$ must be negative to ensure the positive definiteness of the density matrix, which means $\mathrm{Im}(a_c) \leqslant 0$, or equivalently, the inverse scattering length a_c^{-1} is restricted in the upper half complex plane.

With the renormalization relation, one can calculate the two-body scattering t-matrix with energy E,

$$t_2(E) = \frac{2\pi}{m_r} \frac{1}{a_c^{-1} - \sqrt{-2m_r E}}. \tag{3}$$

Note that the negative real axis is taken as the branch cut of $\sqrt{\cdot}$. When $\mathrm{Re}(a_c^{-1}) \geqslant 0$, there is a pole at $E_d = -1/(2m_r a_c^2)$, representing that the system can support a two-body bound state with energy E_d [50].

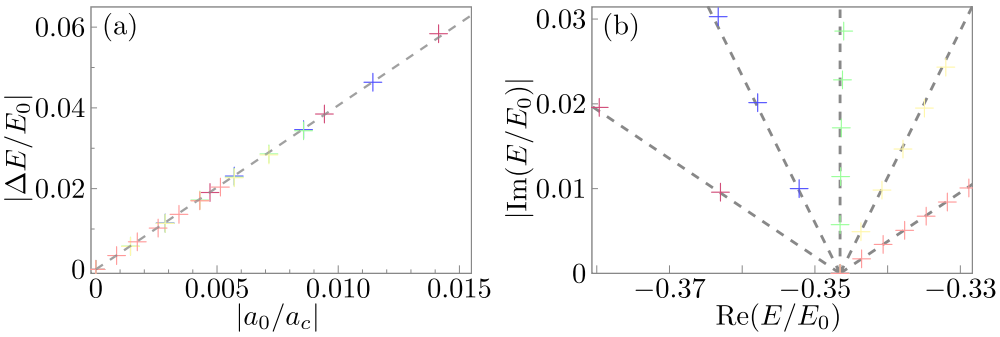

FIG. 2. (a) $|\Delta E| \equiv |E - E(0)|$ as functions of $|a_c^{-1}|$, different colors correspond to different arguments of a_c^{-1}, including $\phi = \pi/6$ (purple), $\pi/3$ (blue), $\pi/2$ (green), $2\pi/3$ (yellow), and $5\pi/6$ (red). One can see that all the lines collapse on a single ray, indicating $|\Delta E| \propto |a_c^{-1}|$. (b) Energy trajectories near unitarity for different arguments $\phi = \pi/6, \pi/3, \pi/2, 2\pi/3, 5\pi/6$ (black solid) and rays with corresponding direction angles $\pi + \phi$ (red dashed). The plot demonstrates that $\arg(\Delta E) \approx \pi + \phi$.

Based on Eq. (3), one can further derive the s-wave atom-dimer scattering matrix $t_3(p, k; E)$ with the relative incoming and outgoing momenta p, k, and energy E, which can be written as

$$t_3(p,k;E) = \frac{m_0}{2pk}\ln\frac{E - \frac{p^2+k^2}{2m_r} + \frac{pk}{m_0}}{E - \frac{p^2+k^2}{2m_r} - \frac{pk}{m_0}} - \int_0^\Lambda \frac{dq}{2\pi^2} q^2 \frac{m_0}{2pq}\ln\frac{E - \frac{p^2+q^2}{2m_r} + \frac{pq}{m_0}}{E - \frac{p^2+q^2}{2m_r} - \frac{pq}{m_0}} \times t_2\left(E - \frac{q^2}{2m_{AD}}\right) t_3(q,k;E). \quad (4)$$

Here, Λ is the momentum cutoff, and $m_{AD} = m_b(m_0 + m_b)/(m_0 + 2m_b)$ is the reduced mass for atom-dimer scattering. Equation (4) can be viewed as the corresponding dissipative STM equation in the presence of two-body losses [2,44]. Similar to t_2, the poles of t_3 on the complex energy plane denote three-body bound states. In the following, we take the ^{133}Cs - ^{133}Cs - ^{6}Li as a concrete example to calculate the whole energy spectra of trimers in the presence of two-body losses.

III. RESULTS

The non-Hermitian trimer energies are in general complex functions of inverse complex scattering length a_c^{-1}, which may be tuned across the upper half complex plane via the optical Feshbach resonance. It is thus natural to choose the argument and modulus of a_c^{-1} as independent tuning parameters, as it gives a much more clear picture of the complex structures of the energy functions. In the following, we demonstrate our numerical results in detail.

A. Trimer energies near unitarity

Around the unitary, if one checks the energy trajectories in Fig. 1, one can see that the trajectories approximately lie on rays with angle $\pi + \phi$ for different $\phi = \arg(a_c^{-1})$ [51]. This behavior implies the existence of a generalized Tan's contact C [47,48], which can be defined as ($\hbar = 1$)

$$\frac{dE}{da_c^{-1}} = -\frac{1}{16\pi m_r} C. \quad (5)$$

Given this formula, the trimer energies around the unitarity can be expressed as

$$\Delta E \approx -\frac{1}{16\pi m_r} C(0) a_c^{-1}, \quad (6)$$

where $\Delta E \equiv E - E(0)$ is the trimer energy measured from the Efimov state energy at unitarity and $C(0)$ denotes the generalized contact at $a_c^{-1} = 0$. We thus conclude that $|\Delta E| \propto |a_c^{-1}|$ and $\arg(\Delta E) \approx \pi + \phi$. Both relations are demonstrated in Fig. 2.

It is worth mentioning that the existence of a generalized Tan's contact is nontrivial, as it involves the *complex* derivative of eigenenergy E whose existence requires not only the existence of partial derivatives with respect to $\mathrm{Re}(a_c^{-1})$ and $\mathrm{Im}(a_c^{-1})$, but also that they satisfy the Cauchy-Riemann relations.

B. Two scenarios

If one tunes $|a_c^{-1}|$ away from unitarity, there generally exist two scenarios. Here, we take the argument $\phi = \pi/2$ as an example to investigate the first scenario in Fig. 1. The three lowest branches of dissipative Efimov trimers are shown in Fig. 3. When $|a_c^{-1}| = 0$, there exists a series of conventional Efimov trimers with $\mathrm{Im}(E) = 0$. As $|a_c^{-1}|$ increases, the trimer energies become complex. Note that their imaginary parts are always negative in the presence of two-body losses. The inverse of the imaginary part of E gives a time scale that represents the lifetime of the trimer. While the real parts increase continuously, the imaginary parts exhibit a nonmonotonic behavior and vanish for large enough $|a_c^{-1}|$, where the trimers merge into three-body branch cuts with positive energies. This is owing to the varying two-body loss rate γ, which can be expressed as

$$\gamma = \frac{1}{2\pi m_r} \frac{|a_c^{-1}|}{|a_c^{-1}|^2 + \left(\frac{\Lambda}{\pi}\right)^2}. \quad (7)$$

As one can see, it also displays a nonmonotonic behavior as $|a_c^{-1}|$ increases.

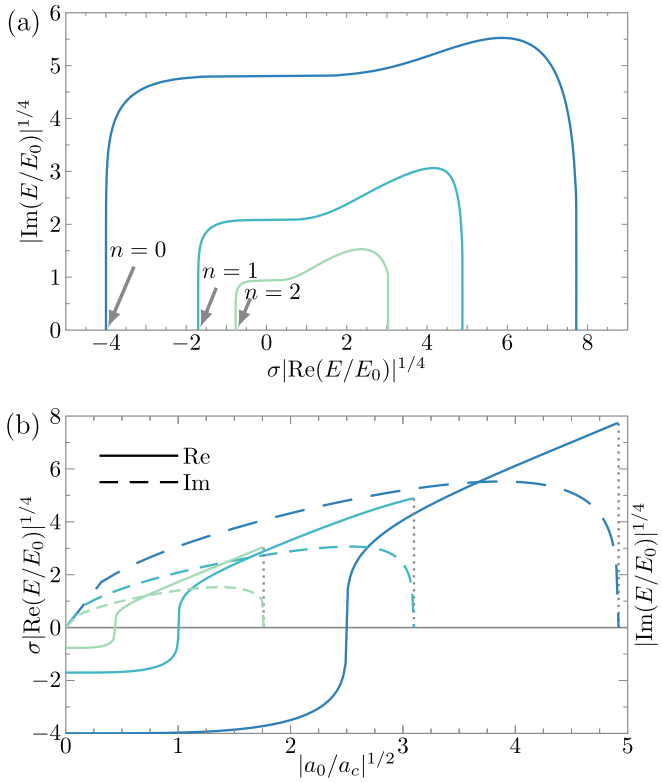

FIG. 3. (a) The energy trajectories start from the three lowest Efimov trimers ($n = 0, 1, 2$) along $\phi = \pi/2$. (b) The real and imaginary parts of trimer energies as functions of $|a_c^{-1}|$ ($\phi = \pi/2$ is fixed). $\sigma \equiv \mathrm{sgn}[\mathrm{Re}(E)]$, $a_0 \equiv 20/\Lambda$ is used as unit length.

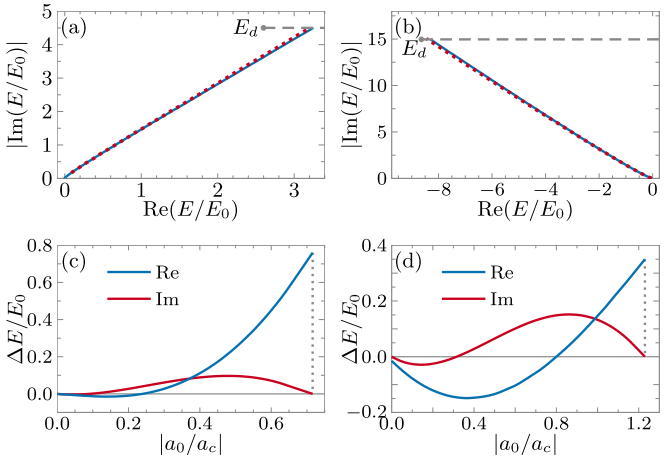

FIG. 4. First row: Energy trajectories in the complex plane. (a) $\phi = \pi/3$, the trajectories connected to the fifth (blue solid) and the sixth (red dotted) real Efimov bound states. (b) $\phi = \pi/6$, the trajectories connected to the fourth (blue solid) and the fifth (red dotted) real Efimov bound states. Gray dashed lines denote the atom-dimer branch cuts where the trimers disappear at. All red dotted lines are scaled by a factor of $e^{2\pi/s_0} \approx 23.7$ to help demonstrate the generalized radial law [Eq. (8)] [55]. Second row: Real and imaginary parts of $\Delta E = E - E_d$ as functions of inverse complex scattering length $|a_c^{-1}|$ with (c) $\phi = \pi/3$ and (d) $\phi = \pi/6$.

Interestingly, when the trajectories end near the real axis, the imaginary parts of the trimer energies tend to zero, which indicates that the system may have long-lived bound states under dissipation. However, it is worth mentioning that in real atomic gases, the infinitely long lifetimes may be shortened due to other dissipative mechanisms such as one- or three-particle losses that are not taken into account in this model.

Figure 3(a) also shows that different branches of complex Efimov trimers display an intriguing discrete scaling behavior. That is, if we scale both the real and imaginary part of the nth branch by $e^{-2\pi/s_0}$, it matches the $(n+1)$th energy branch. This can be viewed as a complex generalization of the celebrated Efimov's radial law [1,2]. To see this, one may apply the hyperspherical coordinate approach [52] to the three-body problem and consider the hyperspherical adiabatic potential $U(\rho)$, with ρ being the hyperradius. In the region $\Lambda^{-1} \ll \rho \ll |a_c|$, the system can be essentially viewed as at unitarity. As a result, the different hyperspherical adiabatic channels are decoupled in this region and the lowest potential channel is $U(\rho) = -(s_0^2 + 1/4)/(2\rho^2)$. Therefore, the solutions to the three-body problem possess the following radial law:

$$a_c^{-1} \to e^{-\pi/s_0} a_c^{-1}, \quad E \to e^{-2\pi/s_0} E, \tag{8}$$

if one follows the conventional argument for the Efimov radial law [1,2]. Similar results have been obtained by calculations through Born-Oppenheimer approximation and adiabatic hyperspherical approximation [39].

Another interesting feature is the existence of trimers with the real parts of their energies beyond the three-body scattering threshold [$\mathrm{Re}(E) > 0$]. Since the system does not support two-body bound states at $\phi = \pi/2$, the only branch cut on the complex energy plane is the positive real axis $\mathbb{R}^+$ [53]. Thus, all the energy trajectories must end on the positive real axis if the energy trajectories are continuous. This allows trimers with the real parts of energies exceeding zero while with nonvanishing imaginary parts.

Indeed, as displayed in Figs. 1 and 3, when the real parts are equal to zero, the trimers do not vanish at the three-body scattering threshold as in the conventional Efimov effect. Moreover, the system can even support a series of trimers with energies that have positive real parts and very small imaginary parts. These long-lived bound states are purely dissipation induced and the mechanism is completely different from other positive energy bound states such as the bound state in the continuum [54].

For $\phi < \pi/2$, the system supports a two-body heavy-light bound state with complex energy $E_d = -1/(2m_r a_c^2)$. And we find that the behavior of the energy trajectories changes qualitatively, even though different energy branches still show the generalized Efimov radial law [Eq. (8)] as demonstrated in Figs. 4(a) and 4(b). Taking $\phi = \pi/3$ and $\phi = \pi/6$ as examples, one can see that the trimer energies exhibit the same feature by plotting $\Delta E = E - E_d$ as functions of $|a_c^{-1}|$ [see Figs. 4(c) and 4(d)]. The real part of ΔE first decreases and then increases to a positive value, while the imaginary part displays an approximate S-shape, with two zero-value ending points. In contrast, the dissipative Efimov branches do not disappear at the atom-dimer scattering threshold, but at atom-dimer branch cut with finite scattering energies.

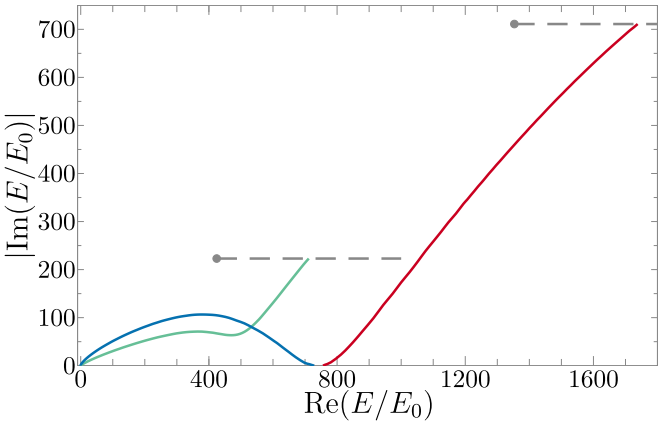

FIG. 5. Deep bound states at $\phi \approx 0.423\pi$. The third lowest Efimov branch (blue) ends on real axis with $\mathrm{Im}(E) = 0$, while the fourth one (green) ends at an atom-dimer branch cut with $\mathrm{Im}(E) \neq 0$. There exists another branch (red) near the blue sold line, which starts from three-body branch cut with $\mathrm{Im}(E) = 0$ and ends at the atom-dimer branch cut with $\mathrm{Im}(E) \neq 0$. Gray dashed lines denote the atom-dimer branch cuts.

In particular, $|\mathrm{Im}(E)| < |\mathrm{Im}(E_d)|$ for large $|a_c^{-1}|$, which means the trimer states have longer lifetimes than the dimers in this region. This effect is quite counterintuitive as it implies that a two-body system can become more stable and long-lived by adding a third particle even in the presence of two-body losses. To understand this result, we adopt the Born-Oppenheimer approximation and calculate the light particle induced effective potential $V_{\mathrm{eff}}(R)$ between the two heavy particles. Note that the imaginary part of V_{eff} can be viewed as an effective two-body loss induced by the light particle. Indeed, we find that it is possible to have $|\mathrm{Im}(V_{\mathrm{eff}})| < |\mathrm{Im}(E_d)|$ in some regions, which suggests that the effective loss rate in a three-body system might be even smaller than the rate in a two-body system. We argue that this is a quantum mechanic effect that arises from the interference of the light particle wave functions (see Sec. IV).

C. Deep bound states

It is worth noting that the two scenarios discussed above only apply to low-energy shallow bound states $[|E| \ll \Lambda^2/(2m_r)]$. For deeper-bound states with energy $|E| \gtrapprox \Lambda^2/(2m_r)$, the system is more complex and nonuniversal as the effect of momentum cutoff becomes more and more important. When the argument ϕ is slightly smaller than $\pi/2$, several deepest energy branches do not vanish into the atom-dimer branch cut continuously, but break down into two branches near the positive real energy axis, as displayed in Fig. 5. The branch that connected to the regular dissipationless Efimov state ends at the three-body branch cut, while the other deep bound state appears slightly above it along the real axis, which further extends to the complex plane and eventually disappears into the atom-dimer branch cut. In fact, for the nth Efimov branch, there exists a critical argument $\phi_c^{(n)}$. The two branches disconnect when $\phi > \phi_c^{(n)}$, while they connect to each other and form one branch when $\phi \leqslant \phi_c^{(n)}$. We note that, in a certain sense, the two branches are not actually disconnected, but only appear to be, as part of the energy trajectory moves into another branch of the Riemann surface [53] while $\phi > \phi_c^{(n)}$. As n increases, the critical argument $\phi_c^{(n)}$ increases and converges to $\pi/2$ for $n \to +\infty$. It is worth noting that similar critical argument phenomena also appear in the calculation of Born-Oppenheimer effective potential (see Sec. IV).

IV. BORN-OPPENHEIMER APPROXIMATION

The Born-Oppenheimer approximation provides an intuitive picture for the understanding of few-body physics in a system with separation of scales in particle masses. In our calculated scenario, because of the large difference between the masses of ^{6}Li and ^{133}Cs, we might first solve the single-particle problem of the light ^{6}Li moving in the presence of two fixed heavy ^{133}Cs atoms. The resultant eigenenergy, which we denote by $\epsilon(R)$ because it is a function of the distance R between two ^{133}Cs atoms, can then be treated as an effective potential between the two heavy particles [2,4].

The Schrödinger equation for the light particle is given by

$$-\frac{\hbar^2}{2m}\nabla_{\mathbf{r}}^2\psi(\mathbf{r}) = \epsilon(R)\psi(\mathbf{r}), \tag{9}$$

where we have assumed that the two heavy particles are located at $-\mathbf{R}/2$ and $\mathbf{R}/2$, which leads to the following boundary conditions:

$$\psi(\mathbf{r}) \approx \frac{1}{\left|\mathbf{r} \pm \frac{\mathbf{R}}{2}\right|} - \frac{1}{a_c}, \quad \mathbf{r} \to \pm\frac{\mathbf{R}}{2}. \tag{10}$$

Because of the parity symmetry of the problem, it is straightforward to show that the solution to Eq. (9) is

$$\psi_{\pm}(\mathbf{r}) = G_\epsilon\left(\mathbf{r} - \frac{\mathbf{R}}{2}\right) \pm G_\epsilon\left(\mathbf{r} + \frac{\mathbf{R}}{2}\right), \tag{11}$$

with

$$G_\epsilon(\mathbf{r}) = \frac{e^{-\kappa r}}{r} \tag{12}$$

being the Green's function. Here we assume $\kappa = \sqrt{-2m\epsilon/\hbar^2}$ with the branch cut of $\sqrt{\cdot}$ defined on the negative real axis.

Substituting this into the boundary conditions, we immediately have

$$t \mp e^{-t} = \frac{R}{a_c}, \tag{13}$$

with $t = \kappa R$.

For closed systems, $a_c \in \mathbb{R}$, Eq. (13) with a minus sign gives a lower bound state energy which can be used to reproduce the Efimov physics in the heavy-heavy-light bound states [2]. Thus, in the following we will focus on the solutions of Eq. (13) with the minus sign.

In Fig. 6, we plot the real and imaginary part of effective potential $\epsilon(R)$ for $\phi = \pi/6$ by numerically solving Eq. (13). We find that $|\mathrm{Im}[\epsilon(\mathbf{R})]| < |\mathrm{Im}(E_d)|$ in some regions. In fact, one can show that $\mathrm{Im}[\epsilon(R)] \approx \mathrm{Im}(E_d) + \frac{1}{m|a_c|R}e^{-R\cos\phi/|a_c|}\sin(\frac{R\sin\phi}{|a_c|} - \phi)$ for $R \gg |a_c|$, which is a function that oscillates around $\mathrm{Im}(E_d)$. Clearly this oscillation arises from the interference between wave functions $G_\epsilon(\mathbf{r} - \frac{\mathbf{R}}{2})$ and $G_\epsilon(\mathbf{r} + \frac{\mathbf{R}}{2})$, which is purely quantum mechanic.

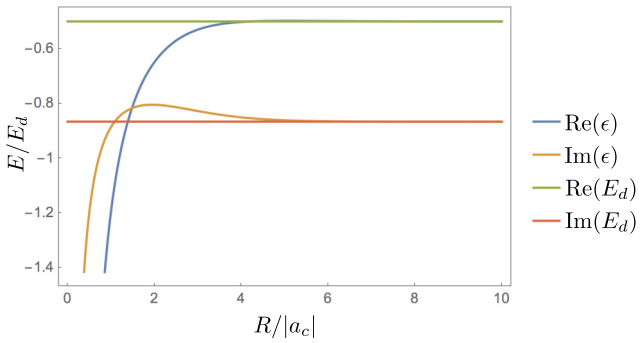

FIG. 6. The real and imaginary part of effective potential $\epsilon(R)$ and two-body bound state energy with $\phi = \pi/6$. $\mathrm{Re}[\epsilon(R)]$ and $\mathrm{Im}[\epsilon(R)]$ tend to $\mathrm{Re}(E_d)$ and $\mathrm{Im}(E_d)$ at large distance but are not always smaller than them like in closed systems.

For a generic ϕ, Eq. (13) either has one or no root with $\mathrm{Re}(\kappa) > 0$, depending on the values of R/a_c. In Fig. 7, we have plotted the boundary between the one-root region (labeled by $n = 1$) and the no-root region (labeled by $n = 0$). We find that, for $\phi = \arg(a_c^{-1}) < \phi_c^{(1)} \approx 1.26263$, Eq. (13) always has exactly one solution for all $R > 0$, which means that the light particle always induces an effective binding between heavy particles. For $\phi \in [\phi_c^{(1)}, \phi_c^{(2)}) \approx [1.26263, 1.46509)$, Eq. (13) has no solution in a bounded interval around $R/|a_c| = 3$. In this region, the heavy particles tend to bind when they are far apart, but this binding effect induced by the light particle vanishes around $R/|a_c| = 3$. For $\phi > \phi_c^{(2)}$, a second interval near $R/|a_c| = 9$ appears which represents that the binding effect vanishes in it. Similar patterns repeat and more intervals where binding effect vanishes appear at $\phi = \phi_c^{(k)}$, $k = 3, 4, 5, \ldots$ Until $\phi = \pi/2$, we find an infinite number of intervals where Eq. (13) has no solutions. This indicates that $\lim_{k\to+\infty} \phi_c^{(k)} = \pi/2$ and the Born-Oppenheimer approximation fails even for very large R.

The behavior of the Born-Oppenheimer potential $\epsilon(R)$ suggests two kinds of mechanisms for the disassociation of Efimov states in the region $\phi \in (\phi_c^{(1)}, \pi/2)$. For "shallow" bound states, the long-range part of $\epsilon(R)$ plays a significant role, and a bound state may disappear because the Born-Oppenheimer effective potential is not strong enough to support it. In this case, since the long-range limit of the effective potential is the dimer energy $\lim_{R\to+\infty} \epsilon(R) = E_d$, one naturally expects that this shallow bound state disassociates into an atom and a dimer, which suggests that the energy trajectory ends at the atom-dimer branch cut. For "deep" bound states, the short-range detail of the effective potential becomes important. For $\phi \in (\phi_c^{(1)}, \pi/2)$, because the effective potential $\epsilon(R)$ in certain short-range intervals may not have a solution, i.e., the light particle does not provide any binding effect between the heavy ones. A deep bound state can disappear because of these nonbinding intervals and disassociate into three particles. One thus expects that in this case the energy trajectories end at the three-body branch cut. This is consistent with our numerical results based on the three-body STM equation with dissipation.

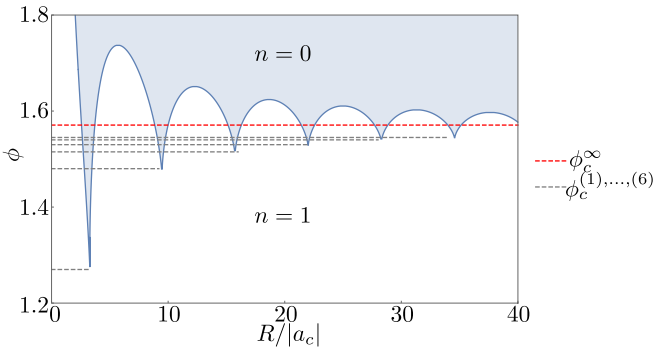

FIG. 7. Number of roots of Eq. (13) (with minus sign) for different argument ϕ and $R/|a_c|$. The equation either has one ($n = 1$) or no root ($n = 0$). There exist a series of critical angles $\phi_c^{(k)}$, $k = 1, 2, \ldots$, with limit value $\lim_{k\to+\infty} \phi_c^{(k)} = \pi/2$. For $\phi \geqslant \pi/2$, the no-solution regions for R tend to infinity, indicating that the Born-Oppenheimer approximation fails even when two heavy particles are far away from each other.

V. CONCLUSIONS AND REMARKS

We study the influence of short-range two-body losses on Efimov bound states. The non-Hermiticity leads to a series of distinct features with no counterparts in the conventional dissipationless Efimov physics. First, the trajectories of Efimov trimers display a unique discrete scaling behavior in the complex energy plane, which is a complex analog of the celebrated Efimov radial law. Second, the system can support Efimov bound states with positive energies and infinite long lifetimes (assuming dissipative processes other than two-particle loss may be ignored). Third, in some regions, the dissipative three-body system may have an even longer lifetime than the two-body system. Our work opens an avenue toward the study of novel few-body physics in the complex energy plane.

Finally, we comment on the experimental observation of complex Efimov trimers in atomic gases. It is worth noting that all the bound states calculated in this work have a negative imaginary part in their energies. One may argue that it would be difficult to observe any resonance in scattering experiments, because all the physical scattering states should have energies in the form of $E + i\epsilon$ with $\epsilon > 0$ being a positive infinitesimal imaginary part, and these energies are on the opposite side of the branch cut (i.e., the real axis). However, this does not rule out the possibility of observing the scattering resonances in a many-body environment (e.g., atomic gases) where all kinds of scattering processes might happen [56]. For example, in Fermionic systems, it is well known that the infinitesimal imaginary part in the many-body Green's function changes sign when the energy is below the Fermi energy.

ACKNOWLEDGMENTS

We acknowledge inspiring discussions with Xiaoling Cui, Hui Zhai, Ran Qi, Ren Zhang, Lei Pan, and Lihong Zhou. We are also grateful to Biqi Yang for help with the figures. The project was supported by State Key Laboratory of IPOC (BUPT) Grants No. 600119525 and No. 505019124 (M.Y.S.), the NSFC under Grants No. 12004049 (M.Y.S.) and No. 12004115 (Z.Y.S.), and Shanghai Sailing Program Grant No. 20YF1411600 (Z.Y.S.).

[1] V. Efimov, Weakly bound states of three resonantly interacting particles, Yad. Fiz. **12**, 1080 (1970) [Sov. J. Nucl. Phys. **12**, 589 (1971)].

[2] E. Braaten and H.-W. Hammer, Universality in few-body systems with large scattering length, Phys. Rep. **428**, 259 (2006).

[3] C. H. Greene, P. Giannakeas, and J. Pérez-Ríos, Universal few-body physics and cluster formation, Rev. Mod. Phys. **89**, 035006 (2017).

[4] P. Naidon and S. Endo, Efimov physics: A review, Rep. Prog. Phys. **80**, 056001 (2017).

[5] T. Kraemer, M. Mark, P. Waldburger, J. G. Danzl, C. Chin, B. Engeser, A. D. Lange, K. Pilch, A. Jaakkola, H.-C. Nägerl *et al.*, Evidence for Efimov quantum states in an ultracold gas of caesium atoms, Nature (London) **440**, 315 (2006).

[6] T. B. Ottenstein, T. Lompe, M. Kohnen, A. N. Wenz, and S. Jochim, Collisional stability of a three-component degenerate fermi gas, Phys. Rev. Lett. **101**, 203202 (2008).

[7] J. R. Williams, E. L. Hazlett, J. H. Huckans, R. W. Stites, Y. Zhang, and K. M. O'Hara, Evidence for an excited-state efimov trimer in a three-component fermi gas, Phys. Rev. Lett. **103**, 130404 (2009).

[8] M. Zaccanti, B. Deissler, C. D'Errico, M. Fattori, M. Jona-Lasinio, S. Müller, G. Roati, M. Inguscio, and G. Modugno, Observation of an Efimov spectrum in an atomic system, Nat. Phys. **5**, 586 (2009).

[9] N. Gross, Z. Shotan, S. Kokkelmans, and L. Khaykovich, Observation of universality in ultracold ^{7}Li three-body recombination, Phys. Rev. Lett. **103**, 163202 (2009).

[10] S. E. Pollack, D. Dries, and R. G. Hulet, Universality in three- and four-body bound states of ultracold atoms, Science **326**, 1683 (2009).

[11] M. Berninger, A. Zenesini, B. Huang, W. Harm, H.-C. Nägerl, F. Ferlaino, R. Grimm, P. S. Julienne, and J. M. Hutson, Universality of the three-body parameter for efimov states in ultracold cesium, Phys. Rev. Lett. **107**, 120401 (2011).

[12] R. J. Wild, P. Makotyn, J. M. Pino, E. A. Cornell, and D. S. Jin, Measurements of tan's contact in an atomic bose-einstein condensate, Phys. Rev. Lett. **108**, 145305 (2012).

[13] S. Knoop, F. Ferlaino, M. Mark, M. Berninger, H. Schöbel, H.-C. Nägerl, and R. Grimm, Observation of an Efimov-like trimer resonance in ultracold atom–dimer scattering, Nat. Phys. **5**, 227 (2009).

[14] S. Nakajima, M. Horikoshi, T. Mukaiyama, P. Naidon, and M. Ueda, Nonuniversal efimov atom-dimer resonances in a three-component mixture of ^{6}Li, Phys. Rev. Lett. **105**, 023201 (2010).

[15] T. Lompe, T. B. Ottenstein, F. Serwane, K. Viering, A. N. Wenz, G. Zürn, and S. Jochim, Atom-dimer scattering in a three-component fermi gas, Phys. Rev. Lett. **105**, 103201 (2010).

[16] R. S. Bloom, M.-G. Hu, T. D. Cumby, and D. S. Jin, Tests of universal three-body physics in an ultracold bose-fermi mixture, Phys. Rev. Lett. **111**, 105301 (2013).

[17] T. Lompe, T. B. Ottenstein, F. Serwane, A. N. Wenz, G. Zürn, and S. Jochim, Radio-frequency association of Efimov trimers, Science **330**, 940 (2010).

[18] S. Nakajima, M. Horikoshi, T. Mukaiyama, P. Naidon, and M. Ueda, Measurement of an efimov trimer binding energy in a three-component mixture of ^{6}Li, Phys. Rev. Lett. **106**, 143201 (2011).

[19] B. Huang, L. A. Sidorenkov, R. Grimm, and J. M. Hutson, Observation of the second triatomic resonance in efimov's scenario, Phys. Rev. Lett. **112**, 190401 (2014).

[20] S.-K. Tung, K. Jiménez-García, J. Johansen, C. V. Parker, and C. Chin, Geometric scaling of efimov states in a ^{6}Li - ^{133}Cs mixture, Phys. Rev. Lett. **113**, 240402 (2014).

[21] R. Pires, J. Ulmanis, S. Häfner, M. Repp, A. Arias, E. D. Kuhnle, and M. Weidemüller, Observation of efimov resonances in a mixture with extreme mass imbalance, Phys. Rev. Lett. **112**, 250404 (2014).

[22] M. Kunitski, S. Zeller, J. Voigtsberger, A. Kalinin, L. P. H. Schmidt, M. Schöffler, A. Czasch, W. Schöllkopf, R. E. Grisenti, T. Jahnke, D. Blume, and R. Dörner, Observation of the Efimov state of the helium trimer, Science **348**, 551 (2015).

[23] N. Syassen, D. M. Bauer, M. Lettner, T. Volz, D. Dietze, J. J. García-Ripoll, J. I. Cirac, G. Rempe, and S. Dürr, Strong dissipation inhibits losses and induces correlations in cold molecular gases, Science **320**, 1329 (2008).

[24] T. E. Lee, Anomalous edge state in a non-Hermitian lattice, Phys. Rev. Lett. **116**, 133903 (2016).

[25] D. Leykam, K. Y. Bliokh, C. Huang, Y. D. Chong, and F. Nori, Edge modes, degeneracies, and topological numbers in non-Hermitian systems, Phys. Rev. Lett. **118**, 040401 (2017).

[26] H. Shen, B. Zhen, and L. Fu, Topological band theory for non-Hermitian Hamiltonians, Phys. Rev. Lett. **120**, 146402 (2018).

[27] S. Yao and Z. Wang, Edge states and topological invariants of non-Hermitian systems, Phys. Rev. Lett. **121**, 086803 (2018).

[28] Z. Gong, Y. Ashida, K. Kawabata, K. Takasan, S. Higashikawa, and M. Ueda, Topological phases of non-Hermitian systems, Phys. Rev. X **8**, 031079 (2018).

[29] K. Kawabata, K. Shiozaki, M. Ueda, and M. Sato, Symmetry and topology in non-Hermitian physics, Phys. Rev. X **9**, 041015 (2019).

[30] N. Okuma and M. Sato, Topological phase transition driven by infinitesimal instability: Majorana fermions in non-Hermitian spintronics, Phys. Rev. Lett. **123**, 097701 (2019).

[31] A. Ghatak and T. Das, Theory of superconductivity with non-Hermitian and parity-time reversal symmetric Cooper pairing symmetry, Phys. Rev. B **97**, 014512 (2018).

[32] K. Yamamoto, M. Nakagawa, K. Adachi, K. Takasan, M. Ueda, and N. Kawakami, Theory of non-Hermitian fermionic superfluidity with a complex-valued interaction, Phys. Rev. Lett. **123**, 123601 (2019).

[33] L. Zhou and X. Cui, Enhanced fermion pairing and superfluidity by an imaginary magnetic field, iScience **14**, 257 (2019).

[34] R. Bouganne, M. Bosch Aguilera, A. Ghermaoui, J. Beugnon, and F. Gerbier, Anomalous decay of coherence in a dissipative many-body system, Nat. Phys. **16**, 21 (2020).

[35] L. Pan, X. Chen, Y. Chen, and H. Zhai, Non-Hermitian linear response theory, Nat. Phys. **16**, 767 (2020).

[36] M. Nakagawa, N. Tsuji, N. Kawakami, and M. Ueda, Dynamical sign reversal of magnetic correlations in dissipative hubbard models, Phys. Rev. Lett. **124**, 147203 (2020).

[37] Y. Ashida, Z. Gong, and M. Ueda, Non-Hermitian physics, Adv. Phys. **69**, 249 (2020).

[38] M. Iskin, Non-Hermitian BCS-BEC evolution with a complex scattering length, Phys. Rev. A **103**, 013724 (2021).

[39] L. Zhou and X. Cui, Effective scattering and Efimov physics in the presence of two-body dissipation, Phys. Rev. Res. **3**, 043225 (2021).

[40] C. Chin, R. Grimm, P. Julienne, and E. Tiesinga, Feshbach resonances in ultracold gases, Rev. Mod. Phys. **82**, 1225 (2010).

[41] C. Wang, C. Liu, and Z.-Y. Shi, Complex contact interaction for systems with short-range two-body losses, Phys. Rev. Lett. **129**, 203401 (2022).

[42] Near an optical Feshbach resonance, it could be shown that the complex scattering length is $a_c = a_{\rm bg}(1 + \frac{\Gamma(I)}{E-\nu-\Gamma(I)+i\gamma/2})$ [40,41], where ν stands for the detuning of the optical field and $\Gamma(I)$ is proportional to the intensity I. This shows that one can in principle tune the complex scattering length across the entire lower half complex plane by adjusting ν and I.

[43] P. Giannakeas and C. H. Greene, Ultracold heteronuclear three-body systems: How diabaticity limits the universality of recombination into shallow dimers, Phys. Rev. Lett. **120**, 023401 (2018).

[44] G. Skorniakov and K. Ter-Martirosian, Three body problem for short range forces. I. Scattering of low energy neutrons by deuterons, Sov. Phys. JETP **4**, 648 (1957).

[45] Y. Wang and B. D. Esry, Universal three-body physics at finite energy near Feshbach resonances, New J. Phys. **13**, 035025 (2011).

[46] T. Hyodo, T. Hatsuda, and Y. Nishida, Universal physics of three bosons with isospin, Phys. Rev. C **89**, 032201(R) (2014).

[47] S. Tan, Large momentum part of a strongly correlated Fermi gas, Ann. Phys. **323**, 2971 (2008).

[48] E. Braaten, D. Kang, and L. Platter, Universal relations for identical bosons from three-body physics, Phys. Rev. Lett. **106**, 153005 (2011).

[49] This is nontrivial as the system may reach unitarity when $\mathrm{Re}(a_c) = 0$ and $\mathrm{Im}(a_c) = -\infty$, which may be regarded as a resonance induced by strong two-body loss.

[50] We note that similar results have been obtained by authors of Refs. [38,39], in which an extra restriction $\mathrm{Re}(E_d) < 0$ is posed. While we find the restriction unnecessary. Indeed, one may find an eigenstate with square integrable wave function $\psi(r) = \frac{e^{-r/a_c}}{r}$ for all the complex scattering length with $\mathrm{Re}(a_c) > 0$, which inevitably results in bound states with energies $\mathrm{Re}(E_d) \geqslant 0$.

[51] Note that in all the figures, we plot $|\mathrm{Im}(E)|$ instead of $\mathrm{Im}(E)$, thus the energy trajectories appear to lie on rays with angles $\pi - \phi$ in the plots.

[52] E. Nielsen, D. Fedorov, A. Jensen, and E. Garrido, The three-body problem with short-range interactions, Phys. Rep. **347**, 373 (2001).

[53] It is worth mentioning that different sides of this branch cut have distinct physical meanings. States below the three-body branch cut, i.e., those states with energies $E - i0^+$, cannot be identified as the usual physical three-body scattering states, but actually correspond to the time reversal of these scattering states. Physically, this is because the boundary condition of the physical scattering states requires their energies to have an infinitesimal positive imaginary part. Mathematically, this can also be understood if one treats the three-body eigenenergy as a multivalued complex function of the inverse scattering length a_c^{-1}. Then the two sides of the three-body (or atom-dimer) branch cut are indeed far away from each other on the Riemann surface defined by this complex function.

[54] V. Neumann and E. Wigner, Uber merkwürdige diskrete eigenwerte, Phys. Z. **30**, 467 (1929).

[55] Note that the momentum cutoff can revise the energy of the several lowest branches, similar to the conventional Efimov effect, which leads to some slight deviation of the discrete scaling law, especially for those states with small n.

[56] This is because the infinitesimal imaginary part in the scattering energy comes from the asymptotic behavior we imposed on the scattering wave function (i.e., an incoming plane wave and an outgoing spherical wave), and this kind of scattering process does not always necessarily happen in a many-body environment.